Quantifying Electric Charge on Cap-Pin Glass Insulator: Investigating the Impact of Pollution through Simulation and Experimental Approaches

Rabie Salhi, Abdelouahab Mekhaldi, Madjid Teguar, and Omar Kherif

Abstract—The objective of this paper is to investigate the behavior of electric charges on cap-pin glass insulator under 50 Hz AC voltage. The study is conducted using COMSOL Multiphysics to understand the charge location, polarity, and parameters affecting their behavior. A 2D-axisymmetric insulator design is used to visualize the overall charges on the insulating system (space charge) and along the insulating surface (surface charge density) under uniform and non-uniform pollution conditions. The research shows that the total charge accumulates over the surface area of the glass material. To quantify the amount of this charge, a simulation method based on using the surface integral of the electric displacement field over this area is introduced, which is supported by experimental tests. Comparing both simulation and experimental results provides insights into the simulation reliability and the parameters' affinity used to those of the real model. Moreover, the simulation helps to identify the critical area where a high amount of charges is accumulated. The findings of this study are presented and examined.

***Keywords*—electric charge, glass insulator, COMSOL, space charge, surface charge density, simulation, charge accumulation.**

NOMENCLATURE

AC	Alternating Current.
2D	Two Dimensional.
HVDC	High Voltage Direct Current.
HVAC	High Voltage Alternating Current.
HV	High Voltage.
ENP	Ecole Nationale Polytechnique.
LRE	Laboratoire de Recherche en Electrotechnique.
SPS	Site Pollution Severity.
IEC	International Electrotechnical Commission.
FEM	Finite Element Method.

I. INTRODUCTION

Electric power consumption has been increasing at a rapid pace worldwide in recent years. In order to meet the growing demand, new power generators must be built, and bulk energy must be transferred. This requires the construction of new overhead transmission lines. Insulators are crucial components of high voltage transmission lines as they provide the dielectric function between live conductors and the structure support, as well as mechanical strength [1]. However, their performance is significantly affected by factors such as material degradation, pollution severity, and different weather conditions (heat, ice, humid air, dust) [2]. Insulator failures can have a severe impact on the electrical power system, so studying and understanding insulator surface behavior is essential, and it requires high attention to ensure their optimal functioning [3].

The premature aging of materials and the occurrence of flashovers in insulators can be related to the accumulation of charge on their outermost surface [4]. These charges play a critical role in determining how the insulator surface interacts with external atmospheric conditions, such as contamination, water droplets, humidity, and others. For this reason, various techniques have been employed to diagnose insulator issues [5]. In recent years, charge distribution analysis techniques have garnered significant interest among researchers [4]. Additionally, several studies have utilized surface charge as a tool to analyze insulators in both HVDC and HVAC systems [6]. The study of charge distribution in insulators has been conducted through both experimental and simulation approaches [4]-[6].

Surface charge is of great interest because it significantly affects the electric field [7]. When the amount of charges flowing to the most contaminated particles located on the insulator surface increases, it can create a high electric field intensity in that location [8]. If this electric field intensity surpasses the breakdown voltage, it can result in a breakdown [7].

Thermal aging diagnosis of polymeric insulators was investigated in [9] using features extracted from space charge accumulation, which is measured in the laboratory using the Pulsed Electro Acoustic system. In [4], a steel mesh was placed around the glass insulator to capture charge accumulation at a distance of 2cm from the insulator edge, which could be useful for monitoring insulators under AC voltages. Laboratory observations have shown that the behavior of electric charge under electric field intensity creates considerable motion activity on water droplets [10]. Understanding these charges can be an effective way to predict insulator aging in the presence of water droplets.

Manuscript received December 24, 2023; revised June 27, 2024.

R. Salhi, A. Mekhaldi and M. Teguar are with the Laboratoire de Recherche en Electrotechnique (LRE), Ecole Nationale Polytechnique (ENP), B.P. 182 El Harrach, Algiers 16200, Algeria. e-mail: (rabie.salhi@g.enp.edu.dz).

O. Kherif is with the Advanced High Voltage Engineering Research Centre, School of Engineering, Cardiff University, Cardiff CF24 3AA, UK. e-mail: (kherifo@cardiff.ac.uk).

Digital Object Identifier (DOI): 10.53907/enpesj.v4xi1. 255

Electrolyte corrosion can significantly affect HV lines during operation. In [11], the authors developed a sophisticated system for in-situ insulator monitoring based on charge to classify corrosion severity.

Simulation-based analysis regarding the electric charge study is one of the most powerful tools to understand and clarify some of the characteristics of insulators found by experimental tests [12]. The results of simulation studies [4],[6] have demonstrated a good correlation with laboratory tests. Furthermore, modeling enables us to illustrate the impact of the amount of charge on the electric field and potential changes [13].

As mentioned earlier, electric charge is closely related to factors like corrosion, temperature, and insulator aging. In this work, we aimed to understand the volumetric and surface charge density, as well as the overall charge on glass insulators, which can significantly impact their behavior. By comparing simulations with experimental data for specific electrical characteristics, such as electric charge, we not only verify the results but also enhance their interpretation and understanding. This approach can also open new research avenues, such as optimization applications, potentially improving the performance of these insulators.

There is a lack of understanding about the distribution of charges on insulating surfaces, particularly for insulators under AC voltages [4]. Therefore, in this paper, we aim to present features that describe the charge characteristics of HVAC insulators. The 1512L cap-pin insulator was used in an experimental investigation conducted at ENP's High Voltage Laboratory under uniform and non-uniform pollution conditions. For both scenarios, we designed and studied a 2D-axisymmetric insulator model using COMSOL software. We investigated space charge accumulation on the glass insulating material, as well as surface charge along the leakage path, and we explained the approach to measuring the waveforms of the charge accumulated on the insulator. This simulation technique for quantifying the global charge has not been done before. We conducted experimental tests to provide a comparative study to validate the simulation results. As a result, we found good agreement between the experimental and simulation tests in terms of the charge waveform, where pollution evaporation was not included

II. Laboratory Test Setup

A. Instruments and Equipment Used

The 1512L cap-pin glass insulator was the main element investigated in this paper. The experiment was conducted at ENP's High Voltage Laboratory (LRE), and the experimental setup diagram is presented in Fig. 1. The system used to perform the tests included the following equipment:

- Contacter and Filter.
- Regulating transformer (380/ 0 to 380 V, 50 kVA, 50 Hz).
- HV Test Transformer (300 kV, 50 kVA, 50 Hz).
- AC capacitive voltage divider with a ratio of 1:1000 ($C_1 = 500$ pF and $C_2 = 0.5\ \mu$ F).
- Measuring capacitor ($C_{\mathrm{m}} = 0.5\ \mu$ F) placed in serie with the insulator.
- Digital oscilloscope to visualize and recorde the charge and the applied voltage waveforms (INSTEK GDS-3504, with 500 MHz of bandwidth).

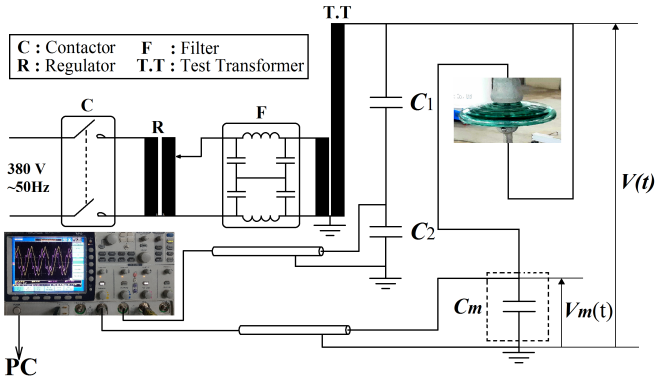

Fig. 1: Laboratory setup diagram

The voltage measured at the capacitor C_{m} terminals, $V_{\mathrm{m}}(t)$, provides information about the charge flow throughout the insulator [14]. The capacitor Cm should be connected in series with the insulator under examination. Based on a previous study [15], it can be noted that the consumption of the oscilloscope can be neglected for the same circuit diagram. The charge over the capacitor has a value so close to the charge over the insulator, with a small error. Therefore, the charge waveform ($Q(t)$) at each instant is measured through the voltage obtained from the oscilloscope as expressed below, where $V(t) \gg V_{\mathrm{m}}(t)$, and C_{in} is the insulator capacitor.

$$Q(t) = C_{\mathrm{m}} V_{\mathrm{m}}(t) = C_{\mathrm{in}}(V(t) - V_{\mathrm{m}}(t)) \approx C_{\mathrm{in}} V(t) \qquad (1)$$

B. Pollution Preparation and Application Procedures

The pollution has been prepared at the ENP's laboratory (LRE). In order to replicate the site pollution severity (SPS) classes, we have adopted in this study the following amounts of NaCl mixed with one liter of distilled water (0, 100, 250, 500 and 750 mg) corresponding to conductivity values respectively 5, 150, 340, 720, 1050 (μS/cm). Those values match to: very light, light, medium, heavy and very heavy as reported on the IEC 60815 standard [16]. Applying the pollution layer on the insulator surface involves using a sprayer, to ensure a uniform layer over the entire surface, The IEC 60507 [17] standard recommends maintaining a distance of 20-40 cm between the sprayer and the insulator surface.

Surface insulators require careful cleanliness before testing. The insulator surface is washed with water and dried with paper, and then cleaned using alcohol (99.8 %) to remove any remaining impurities. After leaving the insulator to dry for a while, the surface is covered with the appropriate pollution solution. Two types of pollution were used in this study: uniform and non-uniform. For the uniform case, the pollutant solution is evenly distributed over the surface using a sprayer fixed at 40 cm distance from the insulator. Six positions on both the upper and lower sides are targeted, and the surface is sprayed three times at each position to ensure full coverage. For the non-uniform case, pollution widths of 5, 10, 15, 20, and 25 cm were applied to the insulator surface starting from the HV side. The electrical conductivity adopted for this case was 1050 μS/cm, corresponding to very heavy pollution.

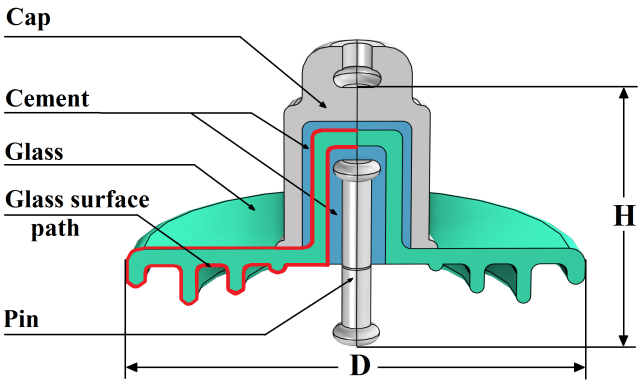

Fig. 2: Insulator model design and parameters

Table. I
MATERIAL PROPERTIES OF THE INSULATOR MODEL [18]

	glass	cap and pin	cement	air
Relative Permittivity ε_r	6	1	15	1.0005
Electric Conductivity σ (S/m)	10^{-14}	10^{4}	10^{-6}	10^{-18}

III. SIMULATION ARRANGEMENT

Our study employs the AC/DC electric current module within the FEM-based COMSOL software to model the 1512L cap-pin insulator. This insulator is composed of several materials, with their main electrical parameters listed in Table. I the value taking of the relative permittivity for the pollution layer is 80. The insulator's design is depicted in Fig. 2, with principal dimensions of Diametre D = 254 mm, Height H = 145 mm. The surrounding air is included in the simulation, with a radius of 2 m, and an extremely fine tetrahedral mesh was used in the simulation geometry to achieve high accuracy .

A time-dependent voltage was conducted in the simulation to simulate real operating conditions. The voltage was applied to the pin while the cap was grounded. To compare the simulation results with those obtained in the laboratory, charge waveform were extracted using the surface integral of the electric displacement field over the glass surface (S) as follows:

$$Q(t) = \iint_S \vec{D}.\mathrm{d}\vec{S} \tag{2}$$

The selection of the integration surface S is of utmost importance as it should encompass the highest accumulation of charge. Visualizing the space and surface charge densities aids in identifying and quantifying these accumulation zones. The detailed steps for determining the targeted surface have been previously outlined in our earlier study [19], where the charge accumulation tracking is presented as flowchart in the fig. 3.

In all simulation operations, the thickness of the pollution layer was determined as follows: for non-uniform pollution, the pollution layer thickness can be selected between 1 and 2 mm [20]. For uniform pollution, the thickness (th_p) was calculated by

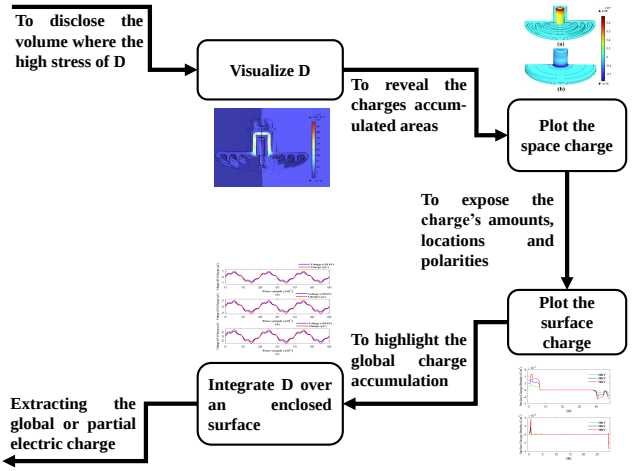

Fig. 3: Flowchart illustrating the quantification of the charge accumulation process [19]

dividing the volume of the pollution (V_p) by the insulator area (S_p) [21]. The surface area of the insulator was obtained using the "geometry surface measurement" feature in COMSOL, which yielded (S_p) = 0.147 m^2. The volume sprayed on the insulator surface was measured to be 15 ml or 1.5$\times$ 10^{-5} m^3, taking into account the volume of runoff that was subtracted from the total volume sprayed.

$$th_p = \frac{V_p}{S_p} = \frac{1.5 \times 10^{-5}}{0.147} \approx 10^{-4} m \tag{3}$$

After several attempts, we found that the simulated charge was a hundred times greater than the experimental charge. This discrepancy is attributed to the fact that the electric current does not flow uniformly through the entire thickness of the insulator. Instead, an effective thickness that contributes to the electrical conduction phenomena was identified. This effective thickness represents only a portion of the total thickness [22], and in our study, it is estimated to be one percent according to the results obtained.

IV. SPACE AND SURFACE CHARGE DENSITIES

The results of space and surface charge densities obtained from the simulation are presented in this section. The glass surface path is divided into two zones: the first is where the glass is bonded to the electrodes by the cement (dielectric-electrode), and the second is along the leakage path where it is in direct contact with the air or covered with pollution (dielectric-air). All results are presented under an applied voltage of 30 kV. Indeed, to present the simulation results, we have focused on the maximum value of the sinusoidal signal rather than the entire waveform. This maximum value, which is 30 kV, represents the peak voltage. At this peak voltage, we observe the maximum charge that can accumulate on the surface of the insulator.

A. *Uniform Pollution Case*

Fig. 4 presents the space charge distribution on the glass material for the upper and lower surfaces, from very light to very high pollution severity. As we can see, positive charges accumulate on the surface area surrounding the HV end. Space charge

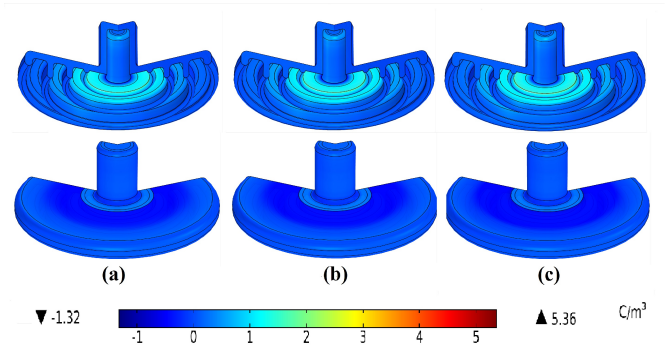

Fig. 4: Space charge distributions for different electrical conductivities, (a) 20 μS/cm, (b) 150 μS/cm, (c) 340 μS/cm.

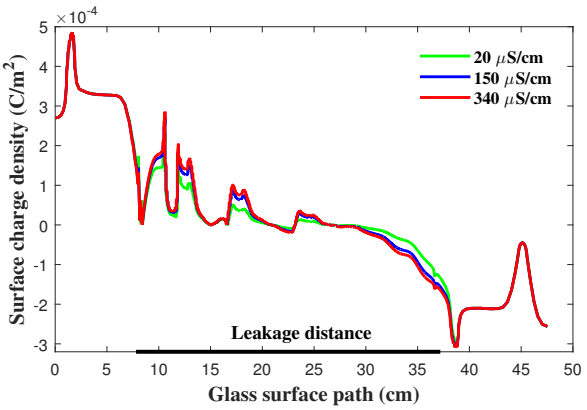

Fig. 5: Surface charge density along the glass surface path for different electrical conductivities.

intensity slightly increases with the increase of the pollution conductivity. For the area belonging to the second zone, high intensity of charge density is observed near the first shed. In fact, this area demonstrates the highest level of temperatures as mentioned in [18]-[23].

Fig. 5 presents the surface charge density along the glass surface path for different electrical conductivities. The charge density distribution along the surface is uneven. In the first zone, we observe that the charge densities are stable and not affected by pollution conductivities, while in the second zone, they are clearly affected by the electrical conductivities of the pollution. The results suggest that increasing the electrical conductivity leads to increased surface charges in the second zone. Along the leakage path, we observed that positive charges accumulate over a distance of 17 cm from the HV end, while negative charges accumulate over the rest of the length. An exceptional peak of positive charge is developed where the smallest distance throughout the glass material is reached between positive charges and the ground (cap).

B. Non-Uniform Pollution Case

Fig. 6 presents the space charge distribution on the upper and lower surfaces of the glass material for different widths of pollution layers. As we can see, positive charges accumulate on the lower surface area of the first zone as well as the area surrounding the HV-end in the second zone for all cases, except for the clean surface case, where charges are confined to the first zone. Negative charges accumulate close to the ground-end on the upper surface.

The fig. 7 presents the surface charge density along the glass surface for different pollution layer widths. The distribution of the surface charge density along the surface is non-uniform. It remains stable in the first zone, while an insignificant change is observed in the second zone, except for the clean surface where it exhibits a different distribution compared to the others, near the high voltage (HV) and ground ends.

However, it reaches high values in the first 5 cm due to the fact that the charges are strongly influenced by both the distance between the two electrodes (HV and ground) and the electrical parameters of the material. The smallest distance between the two electrodes in the insulator is filled with glass material, while the largest distance is filled with air along the leakage distance. Moreover, the electrical conductivity and relative permittivity of

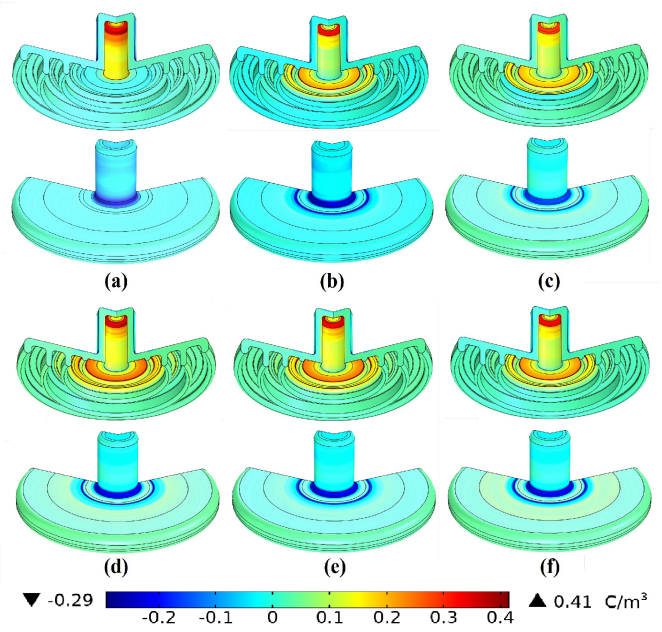

Fig. 6: Space charge distributions for different pollution layer width, (a) clean, (b) 5cm, (c) 10cm, (d) 15cm, (e) 20cm, (f) 25cm

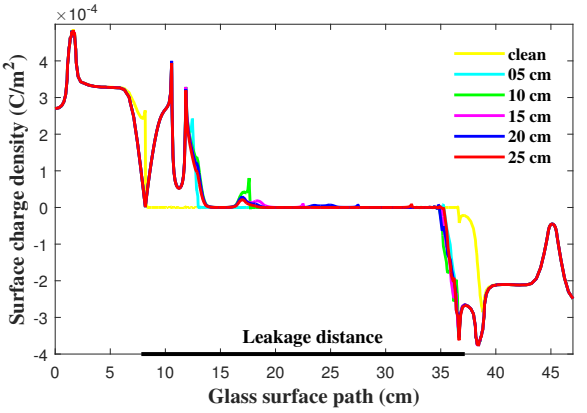

Fig. 7: Surface charge density along the glass surface path for different pollution layer width.

the glass are higher than those of air. These parameters, which impact the charge distribution, are also discussed in [12].

The positive charges accumulate along the 10 cm length starting from the HV-end (5 cm in the case of the pollution width of 5 cm). As for the negative charge, they are trapped in the first 2 cm near the ground end at the dry band surface, where they create an important amount of charges.

V. Charge Waveforms Results

This section presents the global charges in all insulating systems. Tables II and III show the experimental results for flashover voltages under uniform and non-uniform pollution conditions, respectively. We observed that the flashover voltage decreases as either the pollution conductivity or the pollution width increases, leading to a corresponding reduction in the dielectric strength of the insulating system.

To prevent flashover occurrences that could damage the measuring devices, flashover voltages were determined before installing the charge recording setup. Consequently, voltages below the flashover thresholds were used to record the charge waveforms, ensuring that the applied voltages did not exceed 30 kV. However, for a non-uniform pollution width of 25 cm, the voltage had to be reduced to 15 kV due to a flashover event at 25 kV.

Table. II

Flashover voltages for uniform pollution conductivities

Conductivity (μS/cm)	20	150	340
Flashover voltage (kV)	71.5	69	61

Table. III

Flashover voltages for non-uniform pollution widths

Pollution width (cm)	0	5	10	15	20	25
Flashover voltage (kV)	72	70	65	55	35	25

A. *Uniform Pollution case*

The simulation and experimental results of the charge waveforms under a 30 kV applied voltage for various pollution conductivities are presented in Fig. 8. As depicted in the figure, the charge waveforms obtained from both the simulation and experimental tests exhibit a high degree of similarity. Furthermore, the maximum charge value increases as the conductivity value increases. The charge and voltage waveforms are nearly in phase, suggesting that the predominant behavior observed is capacitive.

The charge magnitudes as a function of electrical conductivities of the pollution under different applied voltages are depicted in Fig. 9. As evident from the figure, increasing conductivity values correspond to higher charge magnitudes. Additionally, it is noteworthy that, for the considered voltages and conductivities, the charge magnitude increases with the applied voltages. Furthermore, upon comparing the simulation and laboratory results for the pollution severity levels of very light, light, and medium, the average relative errors between simulation and laboratory are approximately 7.90 %, 5.94 %, and 7.25 %, respectively (as shown in Figure 10). These findings underscore a close agreement between the obtained charge magnitudes in the simulation and laboratory studies.

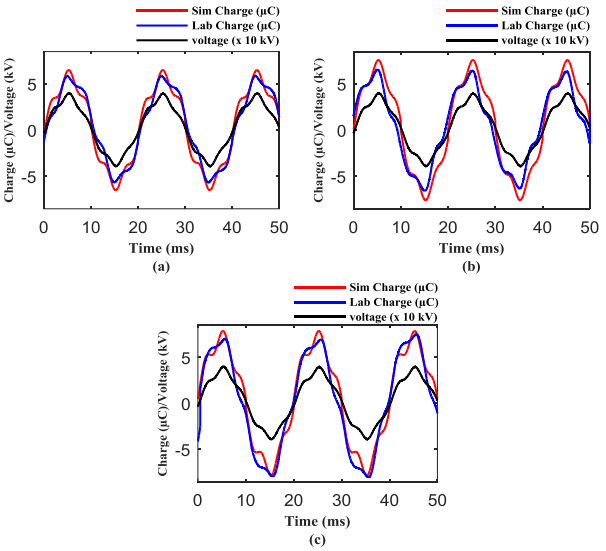

Fig. 8: Charge waveforms for different pollution conductivities: (a) 20 μS/cm, (b) 150 μS/cm, (c) 340 μS/cm.

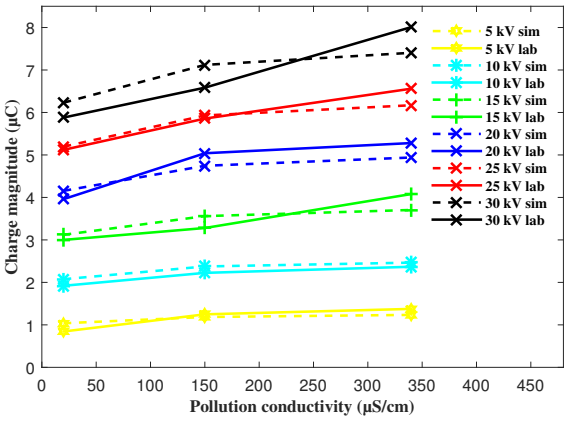

Fig. 9: Charge magnitude versus pollution conductivity for different applied voltages.

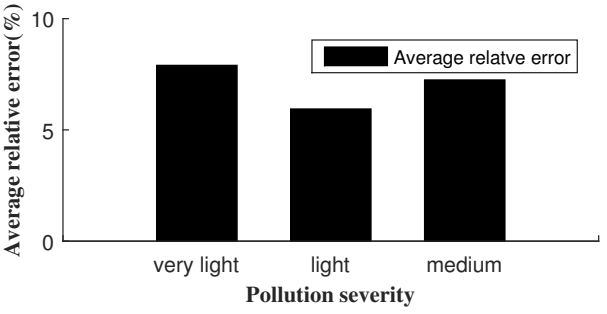

Fig. 10: Average relative error versus pollution severity.

B. *Non-Uniform Pollution Case*

Fig. 11 presents the simulation and experimental results of charge waveforms under a 30 kV applied voltage for the clean surface and various pollution layer widths (5, 10, 15, and 20 cm). Notably, a significant similarity is observed in terms of the charge waveforms between the simulation and experimental

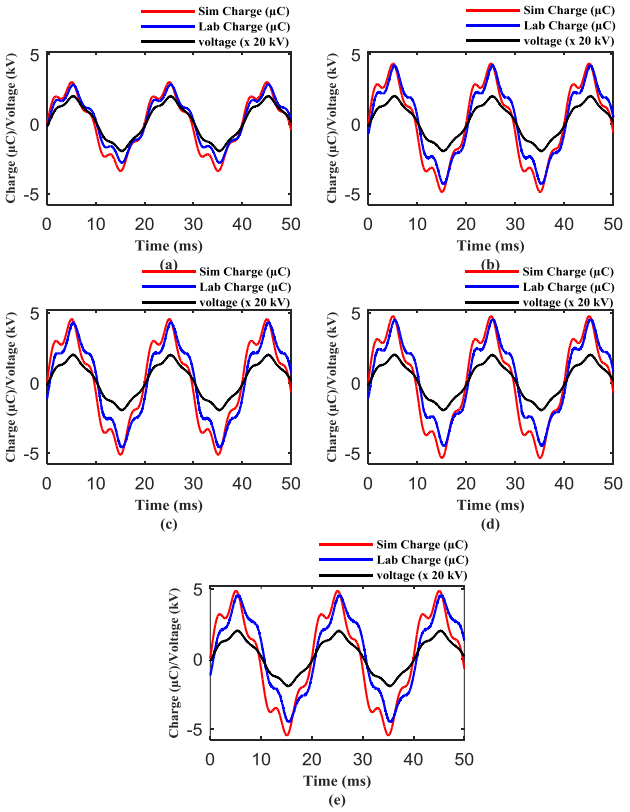

Fig. 11: Charge waveforms for different pollution layer widths (a) clean, (b) 05 cm, (c) 10 cm, (d) 15 cm, (e) 20 cm.

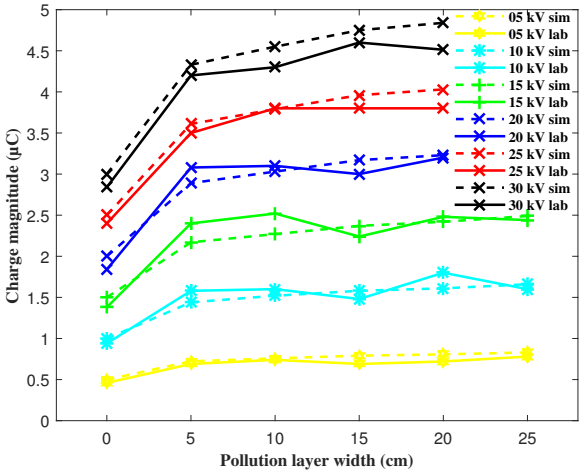

Fig. 12: Charge magnitude versus pollution layer width for different applied voltages.

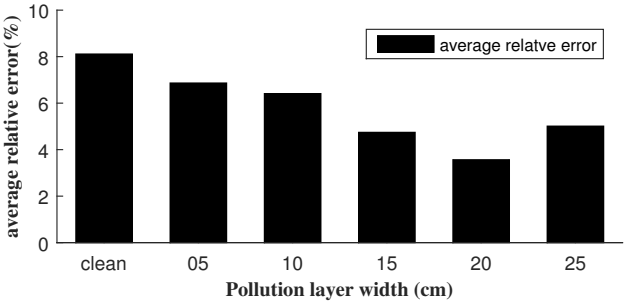

Fig. 13: Average relative error versus pollution layer widths.

results. The presence of the dry band effect leads to the charge and voltage waveforms being almost in phase, indicating the dominant capacitive behavior within the insulating system for all considered pollution widths.

Fig. 12 illustrates the results of charge magnitudes versus pollution layer widths under different applied voltages. From this figure, the results demonstrate a notable increase in charge magnitudes as the pollution layer widths expand, slightly for small voltages and in a significant way for higher voltages. It is possible that this increase is attributed to the initial occurrence of arcing discharges, wherein it contributes, in some way, to the overall charge quantity. The increase in pollution layer width leads to a decrease in arcing voltages, as shown in Table IV, which presents the values of arcing voltages for the pollution layer widths adopted in this study.

It is evident that the charge magnitudes obtained through simulations closely align with those derived from laboratory experiments, with average relative errors of 8.11 %, 6.87 %, 6.41 %, 4.75 %, 3.57 %, and 5.01 % for the clean insulator and pollution widths of 5 cm, 10 cm, 15 cm, 20 cm, and 25 cm, respectively (Figure 13).

To explain why variations in the pollution layer width do not significantly influence the charge variation, it is essential to understand the leakage current circulation between HV and ground ends. This can be illustrated and well explained by current density streamlines, as the leakage current is closely related to the current density. Fig. 14 illustrates the current density as a function of pollution layer width. For a clean insulator, the current density streamlines are concentrated in the radial zone defined by the cap and pin, composed of cement and glass materials (highlighted in red in Fig. 14(a)). However, for all pollution layer widths, a high concentration of current density streamlines is observed through the glass near the end of the cap (black circles in Fig. 14(b) to (f)). Under polluted conditions, the glass thickness has a significantly greater impact on the current density than the surrounding air. This is due to the higher relative permittivity of glass compared to air.

Simulations enable comprehensive analysis of various electrical characteristics, including leakage current. For example, in [24], we investigated the electrical performance of cap-pin and composite insulators used in 400 kV transmission lines. Utilizing the simulation's flexibility, we independently evaluated leakage current through air and insulator materials. Studying the distribution of electric charge takes us a step ahead in understanding additional electrical behaviors. Understanding aspects such as the electric field has assisted us in optimizing the corona ring design [25], thereby enhancing the performance of the cap and pin insulator.

Table. IV
ARCING VOLTAGES VERSUS NON-UNIFORM POLLUTION WIDTH

Pollution width (cm)	0	5	10	15	20	25
Arcing voltage (kV)	48	26	22	18	17	14

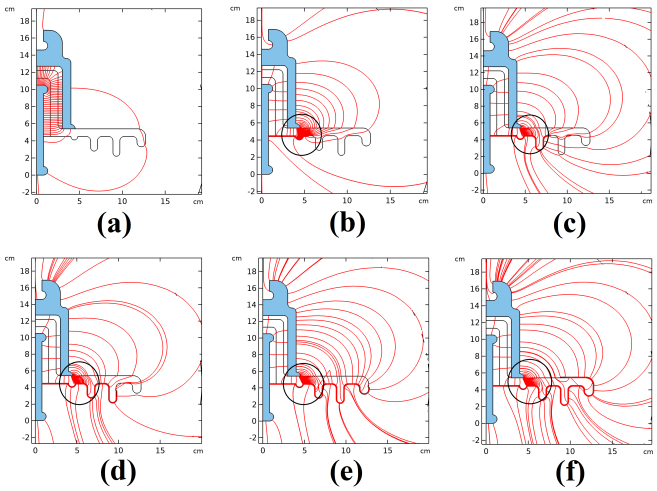

Fig. 14: Current density in function of pollution layer width: (a) clean, (b) 05 cm, (c) 10 cm, (d) 15 cm, (e) 20 cm, and (f) 25 cm.

VI. Conclusion

This research paper focuses on investigating the behavior of electric charges in cap-pin insulator under both uniform and non-uniform pollution conditions. In the case of uniform pollution, different conductivities are selected to represent various pollution severities, including very light (20 μS/cm), light (150 μS/cm), and medium (340 μS/cm). For non-uniform pollution, the study considers different widths of the pollution layer with high conductivity set at 1050 μS/cm. The research employs a combination of simulation and experimental methods to explore these scenarios and gain insights into the location and polarities of the electric charges.

The main findings reveal that the surface charge density in the first zone remains stable, while in the second zone, it varies based on the severity and widths of pollution. Specifically, positive charges accumulate within a distance of 17 cm from the HV electrode in the case of uniform pollution over the second zone. Negative charges, on the other hand, accumulate along the remaining length. For non-uniform pollution over the second zone, positive charges accumulate along a 10 cm length starting from the HV electrode (or 5 cm in the case of a pollution width of 5 cm), while negative charges are confined within the first 2 cm near the ground end.

For both pollution conditions, experimental charge waveforms were recorded with applied voltage level of 30 kV. The results indicate that the magnitudes of the charges increase with the increase in pollution conductivity and also with the increase in pollution layer width. The simulation and laboratory results of the charge waveforms demonstrate good agreement for all the cases considered.

The charge magnitudes obtained from the simulation closely match the experimental results. In the case of uniform pollution, the average relative error is approximately 7.90 % for very light, 5.94 % for light, and 7.25 % for medium pollution severities. Regarding the non-uniform pollution case, the errors are approximately 8.11 % for a clean insulator, and 6.87 %, 6.41 %, 4.75 %, 3.57 %, and 5.01 % for pollution layer widths of 5 cm, 10 cm, 15 cm, 20 cm, and 25 cm, respectively.

Our work focused on understanding the volumetric and surface charge density, as well as the overall charge on glass insulators, which are influenced by factors like corrosion, temperature, and aging. Comparing simulations with experimental data verified our results and enhanced their interpretation. This methodology also opens new research avenues, such as optimization applications, potentially improving insulator performance.

References

[1] R. Salhi, A. Mekhaldi, M. Teguar and O. Kherif, "Corona Ring Improvement to Surface Electric Field Stress Mitigation of 400 kV Composite Insulator," in IEEE Transactions on Dielectrics and Electrical Insulation, vol. 31, no. 3, pp. 1509-1516, June 2024, DOI: 10.1109/TDEI.2023.3342772.

[2] C. Zhang, L. Wang, Z. Guan, and F. Zhang, “Pollution flashover performance of full-scale +- 800 kV converter station post insulators at high altitude area," *IEEE Trans. Dielectr. Electr. Insul.*, vol. 20, no. 3, pp. 717–726, Jun. 2013. DOI: 10.1109/TDEI.2013.6518940.

[3] D. Mussina, A. Irmanova, P. K. Jamwal and M. Bagheri, “Multi-Modal Data Fusion Using Deep Neural Network for Condition Monitoring of High Voltage Insulator," *in IEEE Access.*, vol. 8, pp. 184486-184496, Sept. 2020. DOI: 10.1109/ACCESS.2020.3027825.

[4] N. A. Othman, M. A. M. Piah, Z. Adzis, H. Ahmad, N. A. Ahmad, H. Kamarden, A. A. Suleiman, “Characterization of charge distribution on the high voltage glass insulator string," *Journal of Electrostatics.*, vol. 72, no. 4, pp. 315-321, Aug. 2014. DOI: 10.1016/j.elstat.2014.05.003.

[5] O. E. Gouda, M. M. F. Darwish, K. Mahmoud, M. Lehtonen and T. M. Elkhodragy, “Pollution Severity Monitoring of High Voltage Transmission Line Insulators Using Wireless Device Based on Leakage Current Bursts," *in IEEE Access.*, vol. 10, pp. 53713-53723, May. 2022. DOI: 10.1109/ACCESS.2022.3175515.

[6] J. Mahmoodi, M. Mirzaie and A. A. Shayegani-Akmal, “Surface charge distribution analysis of polymeric insulator under AC and DC voltage based on numerical and experimental tests," *International Journal of Electrical Power & Energy Systems.*, vol. 105, pp 283-296, Feb. 2019. DOI: 10.1016/j.ijepes.2018.08.006.

[7] N. A. Othman, M. A. M. Piah and Z. Adzis, “Charge distribution measurement of solid insulator materials: A review and new approach," *Renewable and Sustainable Energy Reviews.*, vol. 70, pp. 413-426, Apr. 2017. DOI: 10.1016/j.rser.2016.11.237.

[8] L. Yifan, L. Mingzhe, C. Bin, M. Hongwei and W. Liming, “Research on Influence of Charge Quantity of Particles on Contamination Accumulation Characteristics," *2018 IEEE Conference on Electrical Insulation and Dielectric Phenomena (CEIDP)*, Cancun, Mexico, 2018, pp. 211-214, DOI: 10.1109/CEIDP.2018.8544798.

[9] S. Das, J. C. Pandey and N. Gupta, “Space charge diagnostics in aged polymeric insulation," *2013 IEEE 1st International Conference on Condition Assessment Techniques in Electrical Systems (CATCON)*, Kolkata, India, 2013, pp. 395-398, DOI: 10.1109/CATCON.2013.6737535.

[10] J. -M. Löwe and V. Hinrichsen, “Experimental Investigation of the Influence of Electric Charge on the Behavior of Water Droplets in Electric Fields," *2019 IEEE 20th International Conference on Dielectric Liquids (ICDL)*, Roma, Italy, 2019, pp. 1-6, DOI: 10.1109/ICDL.2019.8796707.

[11] D. Yang, F. Yin, H. Mei, L. Wang and C. Guo, “In-Situ Monitoring of Electrolytic Corrosion on the Caps of HVDC Insulators," *in IEEE Sensors Journal.*, vol. 18, no. 20, pp. 8569-8577, Oct. 2018, DOI: 10.1109/JSEN.2018.2865521.

[12] M. Teguar, D. Namane and A. Mekhaldi, "Influence of the thickness and the nature of HVAC insulator model on the flashover voltage and the leakage current," *2013 IEEE International Conference on Solid Dielectrics (ICSD)*, Bologna, Italy, 2013, pp. 186-189, doi: 10.1109/ICSD.2013.6619796.

[13] J. Mahmoodi, M. Mirzaie and A. A. Shayegani-Akmal, "Surface charges on silicon rubber (SiR) insulator and their effect on potential and electric field distribution," *Electr Eng.*, vol. 100, pp. 2695–2705. 2018. DOI: 10.1007/s00202-018-0740-6.

[14] D. D. Dimitriadou, G. K. Soulinaris, P. T. Tsarabaris, C. G. Karagiannopoulos, and P. D. Bourkas, "External Partial Discharges of Pertinax in Air," *Proceedings of the Eighth IASTED International Conference POWER AND ENERGY SYSTEMS (EuroPES 2008)* Corfu, Greece June 23-25, 2008, pp. 313-317.

[15] D. Namane (Ph.D. Dissertation), "Modélisations expérimentale et numérique d'isolateurs HT sous tension alternative 50Hz," Electrical Engineering Department, Electrotechnical Research Laboratory. Alger, Ecole Nationale Polytechnique. Algeria, 2011. D002311

[16] IEC, TS. "60815-1. Selection and Dimensioning of High-voltage Insulators Intended for Use in Polluted Conditions-Part 1: Definitions, Information and General Principles." International Electrotechnical Commission: Worcester, MA, USA (2008). IEC TS 60815-1:2008

[17] IEC Standard 60507,"Artificial pollution tests on high-voltage ceramic and glass insulators to be used on a.c. systems." 2013. IEC 60507:2013.

[18] R. Salhi, A. Mekhaldi, M. Teguar, O. Kherif and M. El Amine Slama, "Cap-Pin glass insulator simulation and leakage current waveform extraction," *2022 2nd International Conference on Advanced Electrical Engineering (ICAEE)*, Constantine, Algeria, 2022, pp. 1-4, DOI: 10.1109/ICAEE53772.2022.9961979.

[19] R. Salhi, A. Mekhaldi, M. Teguar and O. Kherif, "Quantitative Analysis of Electric Charge Distribution on Cap-Pin Insulator Using COMSOL Multiphysics," *Fourth International Conference on Technological Advances in Electrical Engineering (ICTAEE'23)*, Skikda, Algeria, May 2023, pp. 576-579.

[20] A. A. Salem *et al.*, "Pollution Flashover Under Different Contamination Profiles on High Voltage Insulator: Numerical and Experiment Investigation," *IEEE Access*, vol. 9, pp. 37800-37812, Mar. 2021. DOI: 10.1109/ACCESS.2021.3063201.

[21] J. Araya, J. Montaña, and R. Schurch, "Electric Field Distribution and Leakage Currents in Glass Insulator Under Different Altitudes and Pollutions Conditions using FEM Simulations," *in IEEE Latin America Transactions*, vol. 19, no. 8, pp. 1278-1285, Aug. 2021. DOI: 10.1109/TLA.2021.9475858.

[22] M. E. -A. Slama, A. Beroual and H. Hadi, "Influence of the linear non-uniformity of pollution layer on the insulator flashover under impulse voltage - estimation of the effective pollution thickness," *in IEEE Transactions on Dielectrics and Electrical Insulation*, vol. 18, no. 2, pp. 384-392, Apr 2011. DOI: 10.1109/TDEI.2011.5739441.

[23] M. Imran Mousa, Z. Abdul-Malek, Z. Imran Mousa, "Aging Detection of Glass Disc Insulator by Using Infrared Camera," *Indonesian Journal of Electrical Engineering and Computer Science.*, vol. 6, pp. 520-527. 2017. DOI: 10.11591/ijeecs.v6.i3.pp520-527.

[24] R. Salhi, O. Kherif, A. Mekhaldi and M. Teguar, " Electrical Performance of 400-kV Cap-Pin and Composite String Insulators. COMSOL Multiphysics Simulations," *2023 the 23rd International Symposium on High Voltage Engineering (ISH)*, Glasgow, UK, 2023, pp. 260-264, DOI: 10.1049/icp.2024.0483.

[25] R. Salhi, A. Mekhaldi, M. Teguar and O. Kherif, "Optimizing corona ring design for 400 kV cap-pin string insulator to minimize surface electric field under various surface conditions," *2023 International Conference on Electrical Engineering and Advanced Technology (ICEEAT)*, Batna, Algeria, 2023, pp. 1-5, DOI: 10.1109/ICEEAT60471.2023.10426163.

Rabie Salhi received his PhD in Electrical Engineering from Ecole Nationale Polytechnique in July 2024.

Abdelouahab Mekhaldi received the degree of Engineer in 1984 in electrical engineering, the MSc degree in 1990 and a Ph.D. in high voltage engineering in 1999 from Ecole Nationale Polytechnique (ENP) of Algiers. He is currently a Professor at ENP. His main research areas are in discharge phenomena, outdoor insulators pollution, polymeric cables insulation, lightning, artificial intelligence application in high voltage insulation diagnosis and electric field calculation.

Madjid Teguar received the degree in electrical engineering, the master's degree, and the Ph.D. degree in high voltage engineering from the École Nationale Polytechnique (ENP) of Algiers, in 1990, 1993, and 2003, respectively. He is currently a Professor of Electrical Engineering with ENP. His research interests include insulation systems, insulation coordination, earthing of electrical power systems, and polymeric cables insulation.

Omar Kherif received a M.Eng. and Ph.D. degrees in electrical engineering from the Ecole Nationale Polytechnique (ENP) in 2015 and 2019, respectively. He was a mathematical-analysis teacher with ENP from 2016 to 2018. He was also researcher with the Laboratoire de Recherche en Electrotechnique (LRE) of the ENP, where he co-supervised several M.S. theses. He is currently a KTP Associate with Cardiff University and a Technical Consultant with Kingsmill Industries Ltd (UK). His main interests are in high voltage engineering, electromagnetic transients, earthing and power system protection. Dr Kherif is a member of IEEE and some of IEEE societies since 2017